Multifractal Detrended Fluctuation Analysis to Compare Coral Bank and Seafloor Seepage Area-Related Characterization Along the Central Western Continental Margin of India

Bishwajit Chakraborty, *Senior Member, IEEE*, Y. Vishnu Vardhan, K. Haris, Andrew Menezes, S. M. Karisiddaiah, William A. Fernandes, and John Kurian

***Abstract*—In this letter, the characterization of two coral banks is initiated employing the multifractal detrended fluctuation analysis (MFDFA) for multibeam bathymetry and associated backscatter data. The seafloor roughness was estimated using the Hurst exponent of a second-order moment. The two coral banks are located around the buried channels off Malpe, western continental margin of India (WCMI). The Gaveshani bank is lying on a submerged headland with high backscatter strength. The presence of greater seafloor roughness and medium multifractality in the backscatter data series indicates less heterogeneity of the involved process. In an evolutionary process, the Gaveshani bank may not be affected by the paleochannels. Contrary to the Gaveshani bank, another unnamed coral bank located on lowland and with lower backscatter strength shows lower seafloor roughness and greater multifractality, comparatively. This smoothness is due to the considerable heterogeneity of the seafloor process of a paleochannel system. During the Holocene period, the waves and the current action have further modified the morphology of the coral banks. To support the present analysis, we have juxtaposed the multifractal data analysis of seepage and nonseepage seafloor off Goa, WCMI, along with the coral banks.**

***Index Terms*—Backscatter, bathymetry, coral bank, multibeam, multifractal detrended fluctuation analysis (MFDFA), western continental margin of India (WCMI).**

I. Introduction

IN GENERAL, the nature of seafloor processes has shown scale dependence in both temporal and spatial data series [1]. The multibeam data provide concurrent bathymetry and backscatter regarding the large-scale and small-scale roughness. The geology and related topographical data demonstrate the need for a method to simulate the surfaces with a scale-dependent process [2]. In the past, the roughness of the seafloor has been successfully investigated using the fractal dimension parameter for bathymetry profiles [3]–[5].

The fractal dimension measures the degree of fragmentation and irregularities linked to the structure of the data series [6]. The fractals are homogeneous objects having the same scaling properties and are characterized by a single scaling exponent. However, analyzing an inherent property of the signal with only fractal formalism is inadequate. Hence, multifractal formalism (multiscaling properties, and different fractal dimensions) are essential. Multifractal parameters, such as the degree of asymmetry (B), maximum singularity strength (α_0), and degree of multifractality (W) are utilized to differentiate multifractal measures for varied profile data sets [8], [9].

In the western continental margin off Malpe, Karnataka coast, India, two living coral banks were identified using an EM 1002 multibeam echo sounder (MBES), namely, 1) the Gaveshani bank [10] and 2) an unnamed coral bank [11]. The other important provinces in the western continental margin of India (WCMI) are associated with the seafloor seepages [12]. The seepage areas are considered a prospective energy resource for the hydrocarbon accumulations in both shallow and deep environments. Recent studies using MBES system-based data have emphasized the morphological aspects of pockmarks associated with seepage [13], [14].

This letter measures the seafloor roughness, for oceanic coral bank surfaces, to delineate the scale-invariant features in connection with a typical geological seafloor setting. The current work is organized as follows. Section II outlines details of materials and methods, and the study area is given in Section III. In Section IV, a detailed explanation of the methodology of the multifractal detrended fluctuation analysis (MFDFA) is described. The results and discussions of varied geological areas are presented in Section V. Conclusion is provided in Section VI, from the observed results obtained from different geological provinces.

II. Materials and Methods

The MBES data system for the present study was used to acquire a dataset during a survey (in 2006) onboard coastal research vessel (CRV) *Sagar Sukti*. The EM 1002 system operates at a frequency of 95 kHz and acquires the bathymetry

Manuscript received April 10, 2016; revised June 15, 2016; accepted July 23, 2016. Date of publication August 19, 2016; date of current version September 16, 2016. This work was supported in part by the Ministry of Earth Sciences (MoES), New Delhi, India; by the Earth System Science Organization National Centre for Antarctic and Oceanic Research (ESSO–NCAOR), Vasco da Gama, Goa, India; and by the Council of Scientific and Industrial Research National Institute of Oceanography (CSIR–NIO), Dona Paula, Goa, India. This is CSIR-NIO contribution 5924.

B. Chakraborty, Y. V. Vardhan, K. Haris, A. Menezes, S. M. Karisiddaiah, and W. A. Fernandes are with the Council of Scientific and Industrial Research National Institute of Oceanography (CSIR-NIO), Dona Paula 403004, India (e-mail: bishwajit@nio.org; yvardhan@nio.org; harihassainar@gmail.com; amenezes@nio.org; kari@nio.org; william@nio.org).

J. Kurian is with the Earth System Science Organization National Centre for Antarctic and Oceanic Research (ESSO–NCAOR), Vasco da Gama 403804, India (e-mail: john@ncaor.gov.in).

Color versions of one or more of the figures in this paper are available online at http://ieeexplore.ieee.org.

Digital Object Identifier 10.1109/LGRS.2016.2595628

and concurrent backscatter data. The bathymetry data were processed using Neptune software (M/s Kongsberg AS), and the PROBASI II software [15] was used to process the backscatter data. The backscatter strength of the three areas, namely, the Gaveshani bank, 2) the unnamed coral bank, and 3) seepage and nonseepage areas, varied between (−15 to −30 dB), (−32 to −59 dB), and (−26 to −57 dB), respectively. Normally, in the case of a smooth seafloor, the angular backscatter strength displays high values at normal incidence, when compared to the outer beam angles. In the course of a data acquisition, such backscatter strength produced artifacts in the data. On application of the sonar techniques in the preprocessing step along the center beam path, the artifacts were removed. These corrections were utilized to correct values of the outer beam backscatter strength. For image enhancement and gridding, the data were imported to the CFLOOR software version 6.3.1 (M/s Cfloor AS) [13]. Subsequently, a four-stage image processing technique was employed to improve the data image quality [16]. After data processing and image enhancement techniques, a raster-based spatial analysis of data in ArcGIS (M/s ESRI Inc., 1999, USA) was carried out. The study area was arranged as linear data traces (either backscatter or bathymetric) trending in the geographical north–south direction referred to as "profiles." In the present study, 6, 11, and 17 profiles were considered for 1) the Gaveshani bank, 2) the unnamed coral bank, and 3) seepage and nonseepage areas, respectively. The bathymetry and backscatter hold 5970, 27 346, and 7599 data points of all profiles in the three areas, respectively. The sediment grab samples were also considered in and around the bank as a ground truth of the study areas.

III. Study Areas

The Gaveshani bank, a living coral bank [17], is situated approximately 100 km off Karnataka coast along the WCMI (located at latitude 13°24′ N and longitude 73°50′ E). The coral bank lies in the 80-m water depth, with its top surface lying at 38 m below the sea surface (see Fig. 1). Nair and Qasim [10] and Rao *et al.* [18] had reported that the bank has a N–S orientation and is 770 m in length and 330 m in width. A detailed exploration over the bank has yielded calcareous sand, live and dead corals associated with the calcareous algae, mollusks, and serpulids reported from the grab samples [17]. During a second cruise on board R/V Sidorenko [11], another coral bank at about 100 km off the coast in WCMI is also reported. The bank occurs in a water depth of 79 m and is located at latitude 13°43.5′ N and longitude 73°42′ E orientated in the N–S direction. The water depth from the sea surface to the top of the bank is 54 m. The maximum length and width of the bank are about 5900 and 4300 m, respectively. The sediment grab samples contain coral debris and pebbles, in addition to calcareous sand and live and dead corals. In this letter, the MFDFA was carried out as in the previously explored seepage area. We present 17 profiles located at latitude 15°34′ N and longitude 72°50′ E, where water depth varies between 145 and 330 m. Out of these profiles, the seepage area consists of the first eight profiles, and the remaining profiles are the nonseepage area. The seepage area is associated with fault-controlled pockmarks with the fluid escape features in the form of seeps [9]. The composition of the area is coarse sediment associated with the precipitation of diagenetic minerals from the biodegradation of a seepage material [14].

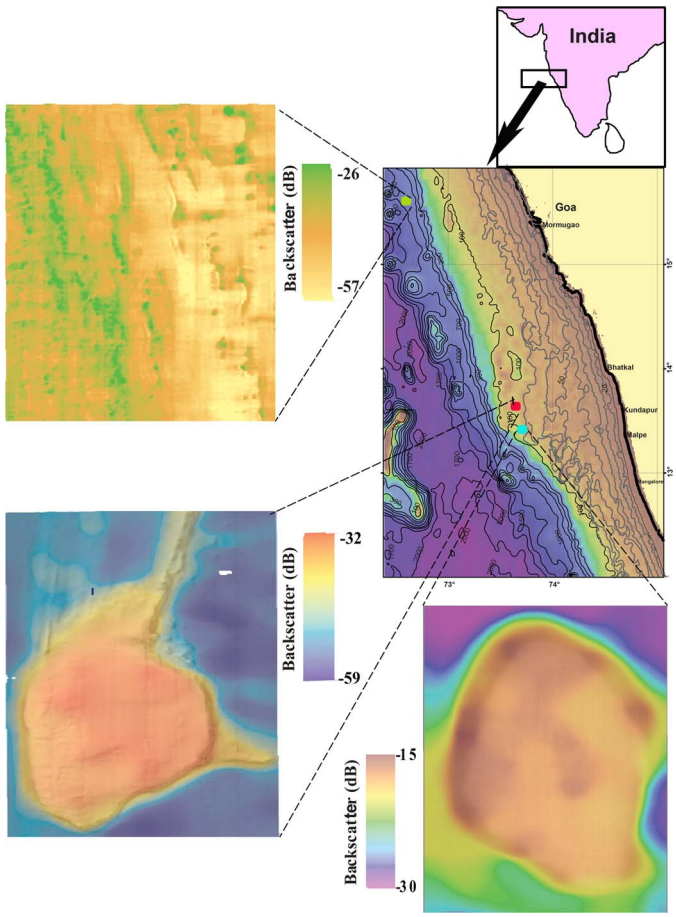

Fig. 1. Locations of the Gaveshani (bottom right), unnamed bank (bottom left), and seepage area (top left).

IV. Methodology of MFDFA

The outline of the MFDFA technique [19]–[21] is concise here. The MFDFA methodology includes five key steps. In the preliminary step, subtracting the mean $\langle x \rangle$ of the bathymetry and backscatter data from the spatial series x_k of length N offers integrated data series $Y(i)$ as follows:

$$Y(i) \equiv \sum_{k=1}^{i} [x_k - \langle x \rangle] \tag{1}$$

where $i = 1, \ldots, N$, and the ensemble average of x is given as follows:

$$\langle x \rangle = \left(\sum_{k=1}^{i} x_k \right) \Big/ N.$$

In the second step, the resultant profile $Y(i)$ is divided into nonoverlapping segments $N_s \equiv \text{int}(N/s)$ of equal length s. Next, in the third step for each of the respective segments, calculation of local trend by using the least square fit is determined using the fitting polynomial $y_v(i)$. The fluctuation function $[F(s, v)]$ is given as follows:

$$F^2(s, v) \equiv \frac{1}{s} \sum_{i=1}^{s} \{Y[(v-1)s + i] - y_v(i)\}^2. \tag{2}$$

Then, the series is detrended by eliminating the fitting polynomial for each segment $v = 1, \ldots, N_s$. Here, the order of fitting considered may be linear, quadratic, cubic, or higher order polynomials. In the fourth step, the average fluctuations

are computed for all the segments to obtain the qth fluctuation order function, as follows:

$$F_q(s) \equiv \left\{ \frac{1}{N_s} \sum_{v=1}^{N_s} \left[F^2(s,v) \right]^{\frac{q}{2}} \right\}^{\frac{1}{q}} \tag{3}$$

where the index variable q can take any real value except zero. The average fluctuations depend on the spatial scales s for a range of qth order (-5 to 5). In the fifth step, the scaling behavior of the fluctuation function is estimated from the slope of plot $\log_2[F_q(s)]$ versus s for a range of q. If the spatial series obeys power law correlations, then the fluctuation order function is expressed as $[F_q(s) \sim s^{h(q)}.]$ Here, the function $h(q)$ is termed as the generalized Hurst exponent. For a stationary signal, the generalized Hurst exponent varies, i.e., $0 < h(q) < 1$. In this case, the generalized Hurst exponent is same as the Hurst exponent $[h(2) = H]$. Correspondingly, for a nonstationary signal, $h(q) > 1$, and the Hurst exponent is needed to correct for a generalized Hurst exponent, i.e., $H = h(2) - 1$, and spectral exponent (β) $[= 2H + 1]$ [22]. However, in the case of a monofractal time series, $h(q)$ is independent of q because the scaling behavior of the variances $F^2(s,v)$ is identical in all the segments v. The average fluctuation of the spatial series gives similar behavior for different orders of q. The qth order signifies the magnifying type, negative values describe small-scale fluctuations, and positive values of a q provide large-scale fluctuations. Through the standard partition function-based multifractal formalism, the Hurst exponent $h(q)$ directly relates to the classical multifractal scaling exponents $\tau(q)$ [19], [21]. The two multifractal scaling exponents are represented in an analytical relation as $[\tau(q) = qh(q) - 1.]$ Another way to characterize a multifractal series is the singularity spectrum $f(\alpha)$ that is related to a $\tau(q)$ via a Legendre transform "$\alpha = \tau'(q)$"; "$f(\alpha) = q\alpha - \tau(q)$." Here, α is termed as the singularity strength or Hölder exponent and measures the regularity of a system at the instantaneous point of the signal, whereas $f(\alpha)$ denoting the dimension of the subset of the series is characterized with α. Using expression of $\tau(q)$, it is also possible to relate α $[= h(q) + qh'(q)]$ and $f(\alpha)$ $[= q[\alpha - h(q)] + 1]$ with $h(q)$. The singularity spectrum $(f(\alpha))$ represents the nature of multifractality, i.e., broader spectrum indicates greater measure of a multifractality denoted by multifractal width $[W = \alpha_2 - \alpha_1]$. The second parameter $(B) = (((\alpha_2 - \alpha_0) - (\alpha_0 - \alpha_1))/\alpha_2 - \alpha_1)$ measures the degree of asymmetry of the inverted parabola curve. It indicates the dominance of low or high fractal exponents. α_0 denotes maximum singularity within the signal.

V. Results and Discussions

A. Results

Here, the multifractal analyses of the coral banks and seepage area from the WCMI, using multibeam data, are carried out. The Hurst exponent plot or singularity spectrum shows typical sigmoid or humped shapes, which illustrate that the profiles are exhibiting multifractality (see Fig. 2). Moreover, the differences in multifractality among the profiles are also noted. The bathymetry profiles of two coral banks show a higher degree of multifractality [see Fig. 2(a) and (c)] than the profiles considered in seepage and nonseepage areas, out of which the lowest multifractality is observed for the nonseepage area (9–17 profiles) of WCMI. In a case of multifractal formalism, the degree of smoothness (or roughness) in the seafloor profile

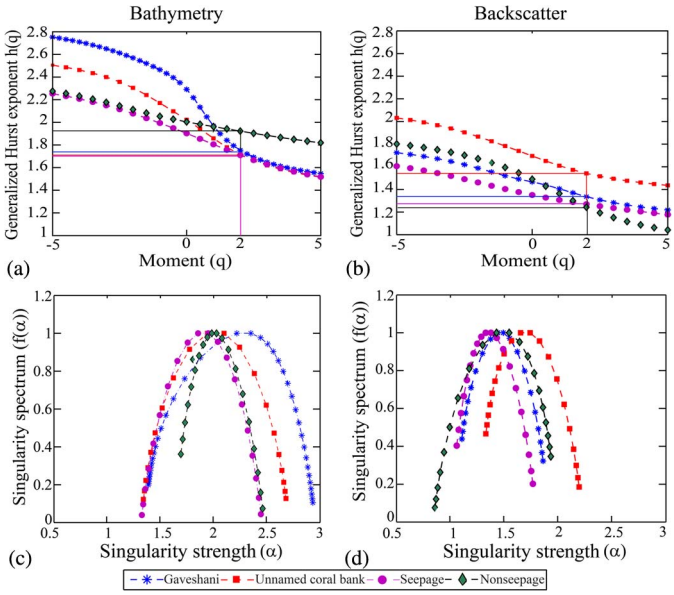

Fig. 2. Multifractal analyses (Hurst exponent and singularity spectrum) of the respective bathymetric and backscatter datasets.

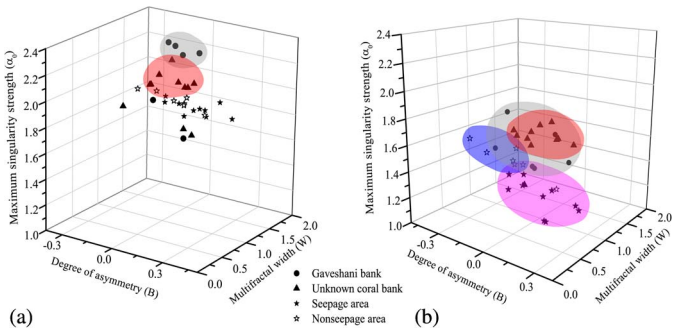

Fig. 3. Multifractal shape parameters (α_0, B & W) are projected in 3-D scatter plot.

can be known with the Hurst exponent of a second-order moment. All the spatial profiles of the bathymetry and concurrent backscatter fall in a nonstationary signal class. Hence, to obtain the roughness, the necessary correction $[H = h(2) - 1]$ is performed. The bathymetry data indicate the structure of the seafloor, and the corresponding backscatter represents the texture of the seafloor. This parameter does not show any important variations (the two coral banks and seepage area have shown the same type of sigmoid trend) throughout its positive q values for seafloor type considered here in this study [see Fig. 2(a)]. Interestingly, the backscatter profiles of the four areas show variation in their roughness. We have also noticed a higher degree of multifractality in a nonseepage backscatter profile of the WCMI than the rest of all the profiles [see Fig. 2(b) and (d)], including coral banks. Thus, the backscatter profiles of the nonseepage area have higher roughness values (0.24), which is sequentially followed by the seepage area (0.27), the Gaveshani bank (0.33), and the unnamed coral bank (0.63) [see Fig. 2(b)].

The results were semi-quantitatively analyzed through multifractal shape parameters, such as maximum (α_0), asymmetry (B), and width (W), estimated for each of the multifractal spectra [9], [21] and then projected on a 3-D scatter plot at the respective three axes [see Fig. 3(a) and (b)]. The bathymetry profiles of the two coral banks show significant clustering in a 3-D scatter plot, with higher values in W and α_0 and moderate B values. These profiles are distinguished from the seepage

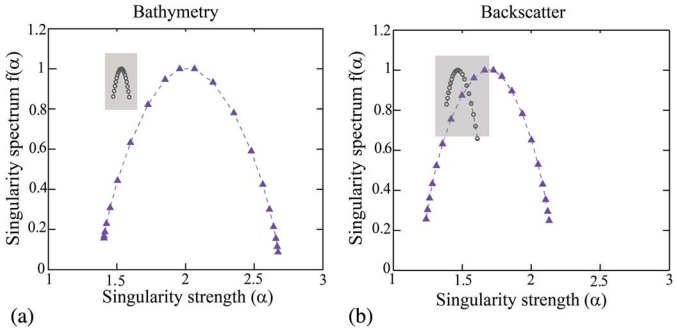

Fig. 4. Test of multifractality (shuffled series (shaded rectangular box) with original series) for bathymetry and backscatter datasets.

and nonseepage areas with moderate values in B and α_0 and lower values in a width W, as illustrated in Fig. 3(a). Prominent clustering was also observed in the backscatter data sets for the coral bank areas. Conversely, the seepage area represents the lowest value for the maximum α_0 [1.24–1.41], which signifies that regular processes are involved in the spatial variability of such signals, i.e., it loses fine structures, and symbolize coarser structures in the multifractal series [8]. For such signals, the degree of asymmetry (B) provides the highest positive values $[-0.07$–$0.31]$, as illustrated in Fig. 3(b), representing a smooth-looking behavior. Correspondingly, the profiles have lower values in the width of the spectrum [0.33–0.80]. Since nonseepage profiles of shallow depth $\sim$ 180 m have a slightly higher value of maximum α_0 [1.25–1.55] than the seepage area, along with low asymmetry B and greater values in width W [0.76–1.26]. It reveals that a complexity exists in the spatial profile series of the nonseepage area. Similar analyses were performed for the backscatter profiles of the two coral banks. The Gaveshani bank shows higher values in α_0 [1.46–1.88] with low to moderate values of W and B. Conversely, at the unnamed coral bank, moderate to high B $[-0.05$–$0.28]$ values are observed along with the higher values in a maximum α_0 and W.

Furthermore, for the entire spatial profiles, there is a need to verify the multifractality only attributed to the long-range correlations. The shuffled series for the bathymetric and backscatter profiles were generated by employing the shuffling procedure [19]. For instance, if the shuffled series exhibits monofractal behavior, i.e., $h_{\text{shuf}}(2) = 0.5$, then, in the shuffling procedure, the long-range correlations present in the series will be destroyed. Each of the spatial scale signals of the bathymetry and their respective backscatter data has shown monofractal behavior [see Fig. 4(a) and (b)]. Thus, all the profiles which exhibit multifractality are due to the long-range correlations only.

B. Discussion

In this letter, the entire spatial signals are exhibiting the nonstationary part of the series. We have applied MFDFA to analyze inherent fluctuations of the signal. The bathymetric data of the Gaveshani bank have the highest degree of multifractality, indicating an inhomogeneous area relief $(1.07 < W < 1.82)$, as compared with an unnamed coral bank $(1.04 < W < 1.47)$. Based on the bathymetry data, the Gaveshani bank displays greater complexity due to the reef structure, implying higher coral growth. The corresponding higher backscatter data show moderate multifractality $(0.58 < W < 0.87)$, i.e., less heterogeneous processes. The Hurst exponent $[h(2)]$ shows higher roughness for backscatter data in the Gaveshani bank. Shuttle Radar Topographic Mission (SRTM) data [see Fig. 5(a)]

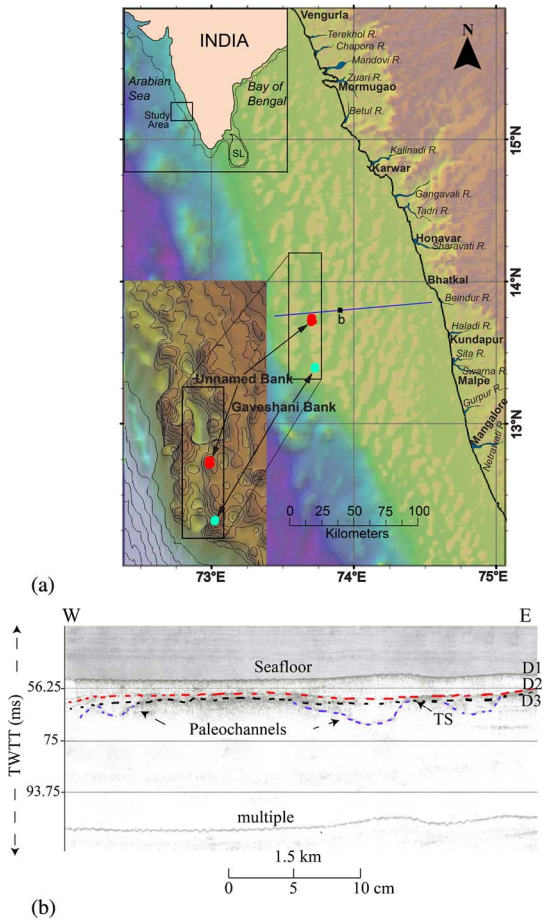

Fig. 5. (a) Site locations with insert bathymetry of SRTM data. (b) shallow seismic record (3.5 kHz) with characteristic near-shore sediments (D1-D3), transgressive surface (TS) and paleochannels.

shows that the Gaveshani bank can be found positioned on the top of a submerged headland, which was unaffected by the paleochannel smoothening effect.

From an unnamed coral bank, in addition to live and dead corals, we have also identified pebbles in the sediment grab samples [11]. The presence of pebble suggests an erosion environment. These pebbles designated, as inland sources of fluvial origin (fanglometric or alluvial deposits), are indicative of earlier in the Holocene period [24]. The coarse quartz pebbles have also been identified in Bundair, Honavar, and Mangalore (near the Netravati River) [25], [26]. In the vicinity of the area, the shallow seismic record shows characteristic near-shore sediments (D1–D3), and the channel fill with the four buried channels or paleochannels overlaid by a transgressive surface (TS) represents a rise in the sea level [27] [see Fig. 5(b)]. Along the Goa and Karnataka coast, these paleodrainage lines link to river courses, which run from the continental shelf to the shelf edge [see Fig. 5(a)]. Ahead of the Holocene period, in a subaerial exposed area, the fluvial deposition was dominant, which smoothens the walls of buried channels. During the transgression period (sea level rise) in the Holocene period, the two coral banks were submerged. Once the bank was flooded, the decrease in the flow of sediment deposition has initiated sediment backfilling along the slope of the channel. Consequently, the hydrodynamics of the area, such as waves and currents, have modified the morphology of the bank. The SRTM data shows an unnamed coral bank submerged located in a low-lying seabed terrain around the paleochannels. The

multifractal results support the geomorphology of the area. The Hurst exponent $[h(2)]$ of an unnamed coral bank backscatter data suggests lower roughness in this region, i.e., smoothened the seafloor along the bank. The smoothened surface also presents lower backscatter strength. The multifractal shape parameter offers a high degree of multifractality $(0.60 < W < 1.08)$. The paleochannel effect and associated coral growth involve heterogeneity of the processes over the unnamed coral bank. This suggests that the unnamed bank has a comparatively less degree of coral growth, as compared with the Gaveshani bank. Seafloor processes are more heterogeneous in nature of unnamed coral bank than the Gaveshani bank.

To cross-validate, we also included seepage and nonseepage areas of WCMI. The seepage area has the highest backscatter strength with low roughness and low multifractality $(0.33 < W < 0.80)$ i.e., less heterogeneous in the process. The backscatter strength is predominantly dominated by acoustic impedance and interface roughness due to the precipitation of diagenetic minerals from the biodegradation of the seepage material, which forms a hard bottom [23]. The nonseepage area has low backscatter strength, higher roughness, and a greater degree of the multifractality [i.e., high heterogeneity in the process $(0.76 < W < 1.26)$]. The reason might be due to intercalation of shell materials along with coarse sediments at the texture level.

VI. Conclusion

In the present study, we have looked at different geological settings in WCMI of two coral bank surfaces. To characterize the necessary geological processes describing seafloor behavior at various spatial scales, we utilized the MFDFA technique. Through using the MFDFA technique, the analysis is performed by using multifractal shape parameters. The two coral banks lie in vicinity to the buried channels off the Karnataka coast, which represent the paleoenvironment originating in WCMI earlier than the Holocene period. The Gaveshani bank displayed higher backscatter strength with comparatively higher roughness. This bank is overlying on the headland and devoid of any fluvial depositional effects. Interestingly, the other unnamed coral bank that is located on a lowland area shows a complexity in the structure of the multifractal series and lower roughness, with the low backscatter strength, in comparison with the Gaveshani bank. This unnamed coral bank displays moderate relief and is a smooth reef. Subsequently, the occurrence of pebbles in this area suggests the erosion effect of paleochannels. To cross-validate, we have included the seepage and nonseepage areas from WCMI in our multifractal analysis. We obtained significant clustering in the estimation of multifractal parameters between coral banks versus the seepage and nonseepage areas.

Acknowledgment

The authors would like to thank to Director Dr. S. W. A. Naqvi, Council of Scientific and Industrial Research National Institute of Oceanography, Goa, India, for his support, and Dr. P. S. Rao, for giving important information in connection with an *unnamed coral bank*. The SRTM data used here are accessed through the web link http://srtm.csi.cgiar.org.

References

[1] B. B. Mandelbrot, "Multifractal measures, especially for the geophysicist," *Pageoph*, vol. 131, no. 1/2, pp. 5–42, Jan./Feb. 1989.

[2] U. C. Herzfeld and C. Overbeck, "Analysis and simulation of scale-dependent fractal surfaces with application to seafloor morphology," *Comput. Geosci.*, vol. 25, no. 9, pp. 979–1007, Mar. 1999.

[3] C. Fox and D. Hayes, "Quantitative methods for analyzing the roughness of the seafloor," *Rev. Geophys.*, vol. 23, no. 1, pp. 1–48, Feb. 1985.

[4] A. Malinverno, "A simple method to estimate the fractal dimension of a self-affine series," *Geophys. Res. Lett.*, vol. 17, no. 11, pp. 1953–1956, Oct. 1990.

[5] B. Chakraborty, R. Mukhopadhyay, V. Mahale, K. Sashikumar, and M. Rajesh, "Fine-scale analysis of shelf-slope physiography across the western continental margin of India," *Geo-Mar Lett.*, vol. 26., no. 2, pp. 114–119, Apr. 2006.

[6] B. Mandelbrot, *Fractals: Form, Chance, and Dimension*. San Francisco, CA, USA: Freeman, 1977.

[7] D. R. Carmichael, L. M. Linnett, S. J. Clarke, and B. R. Calder, "Seabed classification through multifractal analysis of sidescan sonar imagery," *Proc. Inst. Elect. Eng.—Radar, Sonar Navig.*, vol. 143, no. 3, pp. 140–148, Jun. 1996.

[8] L. Telesca, G. Colangelo, V. Lapenna, and M. Macchiato, "Monofractal and multifractal characterization of geoelectrical signals measured in southern Italy," *Chaos, Solitions Fractals*, vol. 18, no. 2, pp. 385–399, Oct. 2003.

[9] B. Chakraborty, K. Haris, G. Latha, N. Maslov, and A. Menezes, "Multifractal approach for seafloor characterization," *IEEE Geosci. Remote Sens. Lett.*, vol. 11, no. 1, pp. 54–58, Jan. 2014.

[10] R. R. Nair and S. Z. Qasim, "Occurrence of a bank with living corals off the south-west coast of India," *Indian J. Mar. Sci.*, vol. 7, no. 1, pp. 54–58, Mar. 1978.

[11] P. S. Rao, "Physiography and depositional environment on the central western continental margin of India," Ph.D. dissertation, Dept. Appl. Geology, ISM, Dhanbad, India, 1995.

[12] L. H. King and B. MacLean, "Pockmarks on the Scotian shelf," *Geol. Soc. Amer. Bull.*, vol. 81, no. 10, pp. 3141–3148, Oct. 1970.

[13] S. Dandapath *et al.*, "Morphology of pockmarks along the western continental margin of India: Employing multibeam bathymetry and backscatter data," *Mar. Petrol. Geol.*, vol. 27, no. 10, pp. 2107–2117, Dec. 2010.

[14] S. Dandapath *et al.*, "Characterization of seafloor pockmark seepage of hydrocarbons employing fractal: A case study from the western continental margin of India," *Mar. Petrol. Geol.*, vol. 29, no. 1, pp. 115–128, Jan. 2012.

[15] W. Fernandes and B. Chakraborty, "Multi-beam backscatter image data processing techniques employed to EM 1002 system," in *Proc. IEEE OES Int. Symp. Ocean Electron.*, Kochi, India, 2009, pp. 93–99.

[16] P. Blondel, *The Handbook of Sidescan Sonar*. Berlin, Germany: Springer-Verlag, 2009, p. 316.

[17] S. Z. Qasim, "Further observations on Gaveshani bank," *Indian J. Mar. Sci.*, vol. 8, pp. 261–262, Dec. 1979.

[18] P. S. Rao, V. N. Koodagali, T. Ramprasad, and R. R. Nair, "Morphology of a coral bank, western continental shelf of India: A multibeam study," *J. Geol. Soc. India*, vol. 41, no. 1, pp. 33–37, Jan. 1993.

[19] J. W. Kantelhardt, S. A. Zschiegner, E. Koscielny-Bunde, S. Havlin, A. Bundeand, and H. E. Stanley, "Multifractal detrended fluctuation analysis of nonstationary time series," *Physica A*, vol. 316, no. 1–4, pp. 87–114, Feb. 2002.

[20] E. A. F. Ihlen, "Introduction to multifractal detrended fluctuation analysis in Matlab," *Front. Physiol.*, vol. 3, no. 141, pp. 1–18, Jun. 2012.

[21] K. Haris, B. Chakraborty, A. Menezes, R. A. Sreepada, and W. A. Fernandes, "Multifractal detrended fluctuation analysis to characterize phase couplings in seahorse (Hippocampus kuda) feeding clicks," *J. Acoust. Soc. Amer.*, vol. 136, no. 4, pp. 1972–1981, Oct. 2014.

[22] M. S. Movahed, G. R. Jafari, F. Ghasemi, S. Rahvar and M. R. R. Tabar, "Multifractal detrended fluctuation analysis of sunspot time series," *J. Statist. Mech.*, vol. 2006, no. 3, pp. 1–7, Feb. 2006.

[23] B. Chakraborty *et al.*, "Application of hybrid techniques (self-organizing map and fuzzy algorithm) using backscatter data for segmentation and fine-scale roughness characterization of seepage-related seafloor along the western continental margin of India," *IEEE J Ocean. Eng.*, vol. 40, no. 1, pp. 3–14, Jan. 2015.

[24] B. R. Manjunatha and K. Balakrishna, "The depositional history of late Quarternary sediments around Mangalore, west coast of India," *Indian J. Marine Sci.*, vol. 28, no. 4, pp. 449–454, Dec. 1999.

[25] M. R. Rao and P. R. Verma, "Palynological investigation of neogene (Early Miocene) sediments of Mangalore Basin, India: Palaeoenvironmental and palaeoclimatic implications," *J. Geol. Soc. India*, vol. 84, no. 1, pp. 55–67, Jul. 2014.

[26] M. Widdowson and Y. Gunnell, *Lateralization, Geomorphology and Geodynamics of a Passive Continental Margin: The Konkan and Kanara Coastal Lowlands of Western Peninsular India*. Oxford, U.K.: Blackwell, 1999. [Online]. Available: https://books.google.co.in/books?id=3Ylftvw0638C&printsec=frontcover#v=onepage&q&f=false

[27] S. M. Karisiddaiah, M. Veerayya, and K. H. Vora, "Seismic and sequence stratigraphy of the central western continental margin of India: Late-Quaternary evolution," *Marine Geol.*, vol. 192, no. 4, pp. 335–353, Sep. 2002.